NIT Intensive Lecture: Nonequilibrium Physics of Amorphous Solids

Instructor: Takeshi Kawasaki

Department of Physics, Graduate School of Science, Nagoya University, Nonequilibrium Physics Laboratory

Last update: September 30, 2024

Download this text

Contents

Contents

Section 1

Syllabus

1. Syllabus

1. Introduction
   - Introduction and Purpose of this Lecture
2. Glass Transition
   - Thermodynamics (Heat Capacity and Entropy)
   - Static Liquid Theory (Static Two-Body Density Correlation Function)
   - Dynamic Liquid Theory (Mean Squared Displacement, Intermediate Scattering Function, Non-Gaussian Parameter (Cumulant Expansion), Four-Point Correlation, Bond Breakage Correlation)
3. Jamming Transition
   - Criticality of Mechanical Variables
   - Isostatic Condition and Criticality of Contact Number
   - Cutting Argument and Criticality of Vibrational Density of States
   - Floppy Modes
   - Nonlinear Rheology of Jamming Systems (Softening and Yielding, Critical Scaling)
4. Nonlinear Rheology of Colloidal Dispersions
   - Langevin Equation and Fluctuation-Dissipation Theorem
   - Flow Curve of Shear Systems (Observation of Glass Transition and Jamming Transition)

Download this text

Contents

Section 2

Introduction and Purpose of the Lecture

2. Introduction and Purpose of the Lecture

Various amorphous solids: Solids formed by cooling or compressing while preventing crystallization.

- Unlike crystals, they have disordered structures and are widely found in everyday life: polar molecules, alloys, inorganic oxides, colloids, powders, cells, etc.
- Thermal systems (atoms, molecules, colloids, cells): **Glass**
- Athermal systems (cells, powders): **Jamming**

Fig. 1: Various amorphous solids

2.1. Purpose of the Lecture

Purpose of the Lecture

- To introduce the basics of liquid theory and nonequilibrium statistical mechanics necessary for the study of amorphous solids.
- In particular, to explain the glass transition and jamming transition in detail.
- After that, to summarize and overview recent advances in research.

Contents

Section 3

Glass Transition

3.1. Introduction

♣ Glass Transition Phenomenon

- The viscosity of a liquid dramatically increases with slight changes in temperature or density (Fig. **2**).
- During this, no significant structural changes are observed using conventional methods such as scattering experiments.
- Unresolved for over 150 years [1].
- This lecture will explain specific analytical methods.

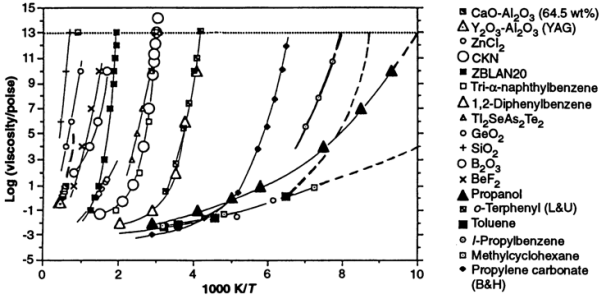

Fig. 2: Temperature dependence of viscosity associated with the glass transition of various substances [2].

3.2. Thermodynamics

In this section, we overview the thermodynamics of crystallization and glass transition, focusing particularly on heat capacity and entropy [2, 3].

Entropy and Heat Capacity

S: Entropy, H: Enthalpy, C_p: Heat capacity at constant pressure, subscripts A, B: States
Under quasi-static constant pressure, a small enthalpy change dH corresponds to heat dQ, so from $dQ = dH = TdS = C_p dT$, integrating over a suitable range gives

$$\Delta S_{A\to B} = \int_{H_A}^{H_B} \frac{dH}{T} = \int_{T_A}^{T_B} \frac{C_p dT}{T}. \tag{1}$$

Simultaneously,

$$C_p = \left(\frac{\partial H}{\partial T}\right)_p = T\left(\frac{\partial S}{\partial T}\right)_p. \tag{2}$$

Heat capacity and entropy behave as follows for crystallization and glass transition (actual data is shown in Fig. **3**).

3.2. Thermodynamics (2)

- Crystallization: First-order transition (Entropy is discontinuous at the melting point T_m, heat capacity diverges (unobservable))
- Glass Transition: Continuous transition (Entropy shows a kink at the glass transition point, heat capacity is discontinuous)

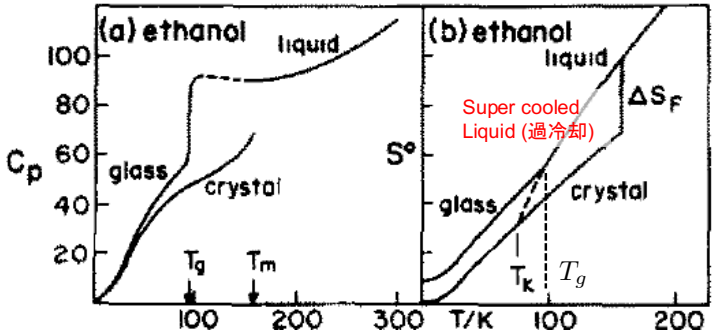

3.2. Thermodynamics (3)

Fig. 3: Heat capacity and entropy (Comparison between crystallization and glass transition) [4]. T_K is the Kauzmann temperature. If a supercooled liquid can be cooled quasi-statically while preventing crystallization, its entropy falls below that of the crystal below T_K (Kauzmann paradox). Since the entropy of the crystal is the minimum, this reversal phenomenon does not occur, and it is thought that a thermodynamic phase transition occurs at T_K.

3.3. Static Liquid Theory: Radial Distribution Function and Static Structure Factor

♣ Density Correlation Function and Radial Distribution Function [5]

The most basic information when investigating the particle structure of a material is the particle density distribution function. The particle density distribution functions are defined as one-body and two-body functions as follows:

$$\rho^{(1)}(\mathbf{r}) = \left\langle \sum_j \delta(\mathbf{r} - \mathbf{r}_j) \right\rangle, \tag{3}$$

$$\rho^{(2)}(\mathbf{r}, \mathbf{r}') = \left\langle \sum_{j \neq k} \delta(\mathbf{r} - \mathbf{r}_j)\delta(\mathbf{r}' - \mathbf{r}_k) \right\rangle. \tag{4}$$

Meanwhile, the two-body density correlation function, normalized by the one-body density function, is defined as the pair distribution function (PDF):

$$g(\mathbf{r}, \mathbf{r}') = \frac{\rho^{(2)}(\mathbf{r}, \mathbf{r}')}{\rho^{(1)}(\mathbf{r})\rho^{(1)}(\mathbf{r}')}. \tag{5}$$

3.3. Static Liquid Theory: Radial Distribution Function and Static Structure Factor (2)

Now consider the two-body correlation function $g(\mathbf{r}+\mathbf{r}', \mathbf{r}')$. Applying this to a system with translational symmetry, noting that $\rho^{(1)}(\mathbf{r}+\mathbf{r}') = \rho^{(1)}(\mathbf{r}') = \rho$, we have

$$\begin{aligned} g(\mathbf{r}+\mathbf{r}', \mathbf{r}') &= g(\mathbf{r}, \mathbf{0}) \\ &= \frac{1}{\rho^2}\left\langle \sum_{j\neq k} \delta(\mathbf{r}+\mathbf{r}'-\mathbf{r}_j)\delta(\mathbf{r}'-\mathbf{r}_k)\right\rangle. \end{aligned} \tag{6}$$

Let $g(\mathbf{r}, \mathbf{0}) =: g(\mathbf{r})$, and performing spatial integration over $\mathbf{r}'$, we get

$$\begin{aligned} \int d\mathbf{r}' g(\mathbf{r}) &= Vg(\mathbf{r}) \\ &= \int d\mathbf{r}' \frac{1}{\rho^2}\left\langle \sum_{j\neq k} \delta(\mathbf{r}+\mathbf{r}'-\mathbf{r}_j)\delta(\mathbf{r}'-\mathbf{r}_k)\right\rangle \\ &= \frac{1}{\rho^2}\left\langle \sum_{j\neq k} \delta(\mathbf{r}+\mathbf{r}_k-\mathbf{r}_j)\right\rangle. \end{aligned} \tag{7}$$

3.3. Static Liquid Theory: Radial Distribution Function and Static Structure Factor (3)

Thus, the pair correlation function considering translational symmetry is

$$\boxed{g(\mathbf{r}) = \frac{1}{\rho N}\left\langle \sum_{j\neq k} \delta(\mathbf{r} - \mathbf{r}_j + \mathbf{r}_k)\right\rangle}. \tag{8}$$

Next, if the particle structure satisfies isotropy, the radial distribution function $g(r)$, which is averaged over a spherical shell with no angular dependence in $\mathbf{r}(r, \theta, \phi)$, is defined as follows:

$$g(r) \quad = \quad \frac{1}{4\pi r^2 \Delta r}\int_r^{r+\Delta r} dr \int_0^{\pi} r d\theta \int_0^{2\pi} d\varphi r \sin\theta g(\mathbf{r}). \tag{9}$$

Next, considering $g(\mathbf{r}) = \frac{1}{N}\sum_j g_j(\mathbf{r})$, the part of the spherical shell integral for $g_j(\mathbf{r})$ represents the number of other particles $\Delta N_j(r)$ within the spherical shell centered on particle j, leading to

$$\boxed{g(r) = \frac{1}{N}\sum_{j=1}^{N} \frac{\left\langle \Delta N_j(r)\right\rangle}{4\pi r^2 \Delta r \rho}}. \tag{10}$$

The expression in Eq. (10) is the most practical, and the results of applying it to liquids, crystals, and glasses are shown in Fig. **4**. From this, it is confirmed that there is significant structural change during crystallization, but there is almost no difference compared to the liquid during glass transition.

3.3. Static Liquid Theory: Radial Distribution Function and Static Structure Factor (4)

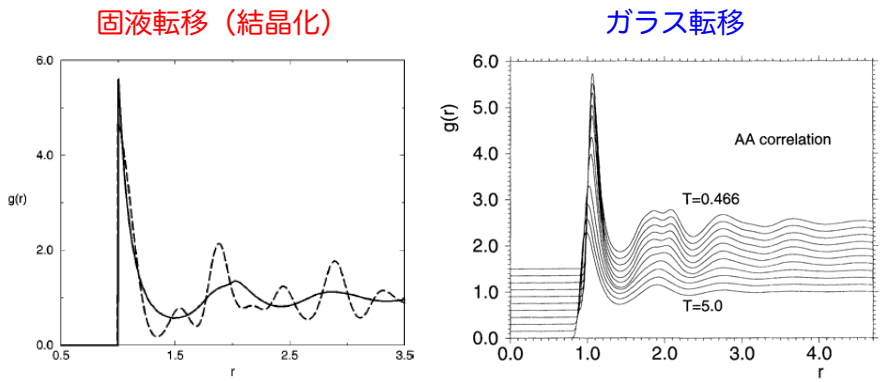

Fig. 4: Radial distribution function $g(r)$ obtained by molecular dynamics simulations. (Left) Solid-liquid transition [6]. (Right) Glass transition [7].

3.3. Static Liquid Theory: Radial Distribution Function and Static Structure Factor (5)

♣ Static Structure Factor

In the analysis of glasses, similar to the behavior of the radial distribution function, there is not much notable change. However, the static structure factor defined below is often used as a structural indicator to capture phase transition phenomena such as phase separation and crystallization:

$$\boxed{S(\mathbf{q}) = \frac{1}{N}\left\langle \delta\tilde{\rho}(\mathbf{q})\delta\tilde{\rho}(-\mathbf{q})\right\rangle}. \tag{11}$$

Here, $\tilde{\rho}(\mathbf{q})$ is the spatial Fourier transform of $\rho(\mathbf{r}) - \rho$:

$$\delta\tilde{\rho}(\mathbf{q}) = \int d\mathbf{r}(\rho(\mathbf{r}) - \rho)e^{-i\mathbf{q}\cdot\mathbf{r}}, \tag{12}$$

where $i = \sqrt{-1}$ and $\mathbf{q}$ is the wavevector. The properties of the static structure factor will be overviewed below. Noting that $\int_V d\mathbf{r}e^{-i\mathbf{q}\cdot\mathbf{r}} = V\delta_{\mathbf{q},\mathbf{0}}$, $\delta\tilde{\rho}(\mathbf{q})$ becomes

$$\delta\tilde{\rho}(\mathbf{q}) = \int d\mathbf{r}\rho(\mathbf{r})e^{-i\mathbf{q}\cdot\mathbf{r}} + N\delta_{\mathbf{q},\mathbf{0}}, \tag{13}$$

3.3. Static Liquid Theory: Radial Distribution Function and Static Structure Factor (6)

so for $\mathbf{q} \neq \mathbf{0}$, using $\tilde{\rho}(\mathbf{q}) = \int d\mathbf{r}\rho(\mathbf{r})e^{-i\mathbf{q}\cdot\mathbf{r}}$, we can also write simply

$$\boxed{S(\mathbf{q}) = \frac{1}{N}\langle\tilde{\rho}(\mathbf{q})\tilde{\rho}(-\mathbf{q})\rangle}. \tag{14}$$

On the other hand, $S(\mathbf{q})$ can also be expressed as a Fourier transform of $g(\mathbf{r})$:

$$\boxed{S(\mathbf{q}) = 1 + \rho\int d\mathbf{r}(g(\mathbf{r}) - 1)e^{-i\mathbf{q}\cdot\mathbf{r}}}. \tag{15}$$

This simple calculation shows the complementary relationship between $g(\mathbf{r})$ and $S(\mathbf{q})$.

Report Assignment (1)

Derive Eq. (15).
(Hint) Consider the sum $\sum_j \sum_k = \sum_{j\neq k} + \sum_{j=k}$ separately.

The limit of $S(\mathbf{q})$ as $\mathbf{q} \to \mathbf{0}$ provides the macroscopic density fluctuation:

$$S(\mathbf{0}) = \frac{V^2}{N}\left\langle(\delta\hat{\rho})^2\right\rangle. \tag{16}$$

3.3. Static Liquid Theory: Radial Distribution Function and Static Structure Factor (7)

Now, in a thermally equilibrated state under isothermal constant pressure, let the volume per particle be $\hat{V}$. Here, the hat notation indicates a fluctuating physical quantity. Replacing density fluctuation with volume fluctuation, we have $\delta\hat{\rho} = \frac{d\rho}{d\hat{V}}\delta\hat{V} = \frac{-N}{\hat{V}^2}\delta\hat{V} = \frac{-\rho}{\hat{V}}\delta\hat{V}$, thus

$$\frac{V^2}{N}\left\langle(\delta\hat{\rho})^2\right\rangle = \frac{\rho}{V}\left\langle(\delta\hat{V})^2\right\rangle. \tag{17}$$

Also, from the fluctuation calculation in statistical mechanics (see [8] Chapter 19),

$$\boxed{\left\langle(\delta\hat{V})^2\right\rangle = -k_{\mathrm{B}}T\left(\frac{\partial V}{\partial P}\right)_T = k_{\mathrm{B}}TV\chi_T}. \tag{18}$$

Here, χ_T is the isothermal compressibility. Summarizing the above, we obtain

$$\boxed{S(\mathbf{0}) = \rho k_B T\chi_T}. \tag{19}$$

Report Assignment (2)

3.3. Static Liquid Theory: Radial Distribution Function and Static Structure Factor (8)

Derive the relation in Eq. (18) under thermal equilibrium.
(Hint) Use the partition function at constant temperature and pressure, $\Upsilon = \sum_j e^{-\beta(U_j + PV_j)}$ (where $\sum_j$ represents the sum over states) and Gibbs free energy $G = -k_B T \log \Upsilon$ [8]. The definition of isothermal compressibility is $\chi_T = -\frac{1}{V}\left(\frac{\partial V}{\partial P}\right)_T$.

3.4. Dynamic Liquid Theory: Mean Squared Displacement, Intermediate Scattering Function, Non-Gaussian Parameter, Four-Point Correlation

♣ Mean Squared Displacement

In two-body density correlation, almost no change is observed during the glass transition, but dramatic changes are seen in the dynamics of particles. The most fundamental quantity in observing dynamics is the mean squared displacement (MSD) of a particle $\Delta\mathbf{r}_j(t) = \mathbf{r}_j(t+t_0) - \mathbf{r}_j(t_0)$ over time t:

$$\left\langle \Delta\mathbf{r}(t)^2 \right\rangle = \frac{1}{N}\left\langle (\mathbf{r}_j(t+t_0) - \mathbf{r}_j(t_0))^2 \right\rangle. \tag{20}$$

For MSD, in the **short-time regime**, we obtain ballistic motion:

$$\left\langle \Delta\mathbf{r}(t)^2 \right\rangle \sim \left\langle v^2 \right\rangle t^2 \sim \frac{k_B T}{m} t^2. \tag{21}$$

In the **long-time regime**, it shows a diffusion process:

$$\left\langle \Delta\mathbf{r}(t)^2 \right\rangle \sim 2dDt, \tag{22}$$

3.4. Dynamic Liquid Theory: Mean Squared Displacement, Intermediate Scattering Function, Non-Gaussian Parameter, Four-Point Correlation (2)

where d is the spatial dimension, and D is the diffusion coefficient.
Figure **5** shows the temperature dependence of a binary mixture of particles of different sizes (Lennard-Jones liquid) obtained by molecular dynamics simulations. Particularly in the low-temperature region, a plateau is observed between the ballistic and diffusive regimes. The plateau in MSD corresponds to the cage vibration in solids, indicating that supercooled liquids are semi-solid (over time, the cage breaks, and the system transitions to diffusion).

3.4. Dynamic Liquid Theory: Mean Squared Displacement, Intermediate Scattering Function, Non-Gaussian Parameter, Four-Point Correlation (3)

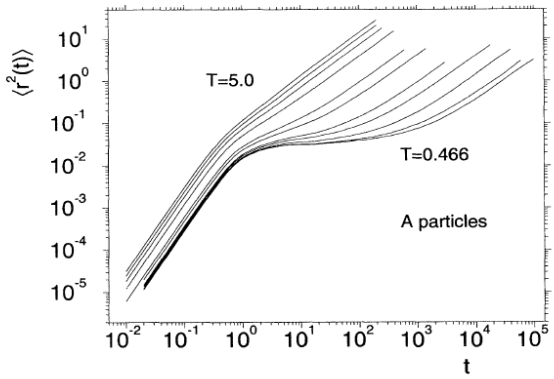

Fig. 5: Temperature dependence of mean squared displacement accompanying glass transition [7].

3.4. Dynamic Liquid Theory: Mean Squared Displacement, Intermediate Scattering Function, Non-Gaussian Parameter, Four-Point Correlation (4)

♣ Intermediate Scattering Function

In addition to the mean squared displacement, the intermediate scattering function defined below is also often used for observing glass transition:

$$F(q,t) = \frac{1}{N}\left\langle \rho(\mathbf{q},t)\rho(-\mathbf{q},0)\right\rangle . \tag{23}$$

Generally, if the magnitude of the wave vector is chosen to be about $2\pi/d$ (d is the average particle diameter), it can capture the relaxation dynamics of particles. Here,

$$\rho(\mathbf{q},t) = \int d\mathbf{r}\sum_j \delta(\mathbf{r}-\mathbf{r}_j)e^{-i\mathbf{q}\cdot\mathbf{r}} = \sum_j e^{-i\mathbf{q}\cdot\mathbf{r}_j(t)}. \tag{24}$$

Thus,

$$F(q,t) = \frac{1}{N}\left\langle \sum_j e^{-i\mathbf{q}\cdot\mathbf{r}_j(t)}\sum_k e^{i\mathbf{q}\cdot\mathbf{r}_k(0)}\right\rangle = \frac{1}{N}\sum_{jk}\left\langle e^{-i\mathbf{q}\cdot\mathbf{r}_j(t)}e^{i\mathbf{q}\cdot\mathbf{r}_k(0)}\right\rangle , \tag{25}$$

3.4. Dynamic Liquid Theory: Mean Squared Displacement, Intermediate Scattering Function, Non-Gaussian Parameter, Four-Point Correlation (5)

and it is known that focusing particularly on the self-term is sufficient. The self-term of the intermediate scattering function is called the self-intermediate scattering function:

$$F_{\mathrm{s}}(q,t) = \frac{1}{N}\sum_j \left\langle e^{-i\mathbf{q}\cdot(\mathbf{r}_j(t)-\mathbf{r}_j(0))}\right\rangle = \frac{1}{N}\sum_j \left\langle e^{-i\mathbf{q}\cdot\Delta\mathbf{r}_j(t)}\right\rangle. \tag{26}$$

The self-intermediate scattering function suggests a relationship with the displacement vector $\Delta\mathbf{r}_j(t)$.

Report Assignment (3)

Show that $F(\mathbf{q},t)$ is a real number.

3.4. Dynamic Liquid Theory: Mean Squared Displacement, Intermediate Scattering Function, Non-Gaussian Parameter, Four-Point Correlation (6)

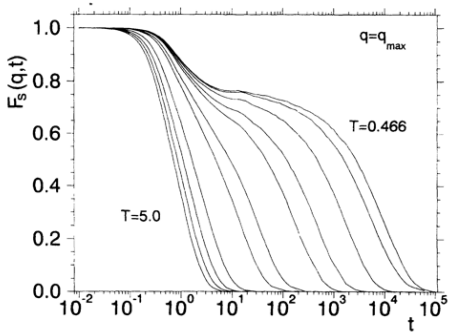

Fig. 6: Temperature dependence of the self-intermediate scattering function accompanying glass transition [9].

3.4. Dynamic Liquid Theory: Mean Squared Displacement, Intermediate Scattering Function, Non-Gaussian Parameter, Four-Point Correlation (7)

Figure **6** shows the temperature dependence of the self-intermediate scattering function accompanying the glass transition. Relaxation from 1 to 0 is observed in all cases, but the relaxation time τ_α (the time satisfying $F_s(q,t) = 1/e$) becomes significantly longer as the temperature decreases. Particularly, the self-intermediate scattering function in **high-temperature liquid state** is given by

$$F_s(q,t) \sim e^{-(t/\tau_\alpha)}. \tag{27}$$

On the other hand, in **low-temperature supercooled liquid**, in the long-time regime, it can be expressed as

$$F_s(q,t) \sim Ae^{-(t/\tau_\alpha)^\beta}, \tag{28}$$

where $\beta < 1$, known as the **stretched β exponent**. The origin of $\beta < 1$ is thought to be one of the factors for dynamic heterogeneity. Also, in some nonequilibrium systems, relaxations with $\beta > 1$ are observed, which are sometimes referred to as **compressed β**.
The behavior in Eq. (27) can be obtained through the following procedure. First, in a high-temperature liquid, the displacement vector $\Delta\mathbf{r}_j(t)$ is assumed to satisfy a Gaussian distribution. Also, assuming isotropy of the system, we can choose the wave vector as $\mathbf{q} = (q,0,0)$ without losing generality to simplify calculations:

$$F_s(q,t) = \frac{1}{N}\sum_j \left\langle e^{-iq\Delta x_j(t)} \right\rangle = \left\langle e^{-iq\Delta x(t)} \right\rangle. \tag{29}$$

3.4. Dynamic Liquid Theory: Mean Squared Displacement, Intermediate Scattering Function, Non-Gaussian Parameter, Four-Point Correlation (8)

In the following, the subscript j is omitted as shown in the above expression. Now, if $\Delta x(t)$ satisfies a Gaussian distribution, the calculation of the average $\langle\cdot\rangle$ is

$$
\begin{aligned}
F_{\rm s}(q,t) &= \left\langle e^{-iq\Delta x(t)} \right\rangle \\
&= \int_{-\infty}^{\infty} d(\Delta x) e^{-iq\Delta x(t)} \sqrt{\frac{1}{2\left\langle \Delta x^2(t) \right\rangle \pi}} e^{-\frac{\Delta x^2}{2\left\langle \Delta x^2(t) \right\rangle}} \\
&= \int_{-\infty}^{\infty} d(\Delta x) e^{-iq\Delta x(t)} \sqrt{\frac{1}{4\pi D t}} e^{-\frac{\Delta x^2}{4Dt}} \\
&= \int_{-\infty}^{\infty} \sqrt{\frac{1}{4\pi D t}} d(\Delta x) e^{-\frac{(\Delta x - 2iDqt)^2 + 4D^2q^2t^2}{4Dt}} \\
&= e^{-q^2 D t} \\
&= e^{-t/\tau_\alpha}. \qquad (30)
\end{aligned}
$$

3.4. Dynamic Liquid Theory: Mean Squared Displacement, Intermediate Scattering Function, Non-Gaussian Parameter, Four-Point Correlation (9)

Here, $\left\langle \Delta x^2(t) \right\rangle = 2Dt$ was used. From this, under Gaussian approximation, the structural relaxation time τ_α satisfies

$$\boxed{\tau_\alpha = 1/Dq^2}, \tag{31}$$

which means it is inversely related to the diffusion coefficient D.

♣ Non-Gaussianity (Cumulant Expansion) [10]

In reality, in supercooled liquids, the displacement distribution becomes heterogeneous, and non-Gaussianity becomes important. This non-Gaussianity can be evaluated using the cumulant expansion below. Now,

3.4. Dynamic Liquid Theory: Mean Squared Displacement, Intermediate Scattering Function, Non-Gaussian Parameter, Four-Point Correlation (10)

$\log \left\langle e^{-iq\Delta x(t)} \right\rangle$ itself is the cumulant generating function, and by expanding around $-iq\Delta x(t)$, where $\mu_m = \langle \Delta x(t)^m \rangle$, we have

$$\begin{aligned}
\log \left\langle e^{-iq\Delta x(t)} \right\rangle &= \log \left\langle \left(1 + \sum_{m=1}^{\infty} \frac{(-iq\Delta x(t))^m}{m!} \right) \right\rangle \\
&= \log \left(1 + \sum_{m=1}^{\infty} \frac{(-iq)^m \mu_m}{m!} \right) \\
&= \sum_{m=1}^{\infty} \frac{(-iq)^m \mu_m}{m!} - \left(\sum_{m=1}^{\infty} \frac{(-iq)^m \mu_m}{m!} \right)^2 /2 + \left(\sum_{m=1}^{\infty} \frac{(-iq)^m \mu_m}{m!} \right)^3 /3 + \cdots \\
&= \frac{(-iq)^2 \mu_2}{2!} + \frac{(-iq)^4 \mu_4}{4!} + \frac{1}{2} \left(\frac{(-iq)^2 \mu_2}{2!} \right)^2 + O(q^6). \qquad (32)
\end{aligned}$$

3.4. Dynamic Liquid Theory: Mean Squared Displacement, Intermediate Scattering Function, Non-Gaussian Parameter, Four-Point Correlation (11)

Here, since the distribution of Δx is symmetric, all odd-order terms of m are dropped. Simplifying the above equation,

$$\begin{aligned}\log\left\langle e^{-iq\Delta x(t)}\right\rangle &= \frac{-q^2}{2}\left\langle\Delta x(t)^2\right\rangle + \frac{q^4}{4!}\left(\left\langle\Delta x(t)^4\right\rangle - 3\left\langle\Delta x(t)^2\right\rangle^2\right) + O(q^6)\\ &= -q^2Dt + \frac{q^4(Dt)^2}{4}\alpha_2(t) + O(q^6),\end{aligned} \tag{33}$$

where the q^2 term corresponds to the Gaussian approximation, and the terms beyond q^4 represent non-Gaussianity. Particularly, the coefficient $\alpha_2(t)$ in the fourth cumulant is called the non-Gaussian parameter:

$$\boxed{\alpha_2(t) = \frac{\left\langle\Delta x(t)^4\right\rangle}{3\left\langle\Delta x(t)^2\right\rangle^2} - 1}. \tag{34}$$

For the d-dimensional displacement $\mathbf{r}(t)$,

$$\boxed{\alpha_2(t) = \frac{d\left\langle\Delta \mathbf{r}(t)^4\right\rangle}{(d+2)\left\langle\Delta \mathbf{r}(t)^2\right\rangle^2} - 1} \tag{35}$$

3.4. Dynamic Liquid Theory: Mean Squared Displacement, Intermediate Scattering Function, Non-Gaussian Parameter, Four-Point Correlation (12)

holds [10].

3.4. Dynamic Liquid Theory: Mean Squared Displacement, Intermediate Scattering Function, Non-Gaussian Parameter, Four-Point Correlation (13)

- Figure **7** shows the temperature dependence of $\alpha_2(t)$ in a supercooled liquid [11]. $\alpha_2(t)$ is 0 in both the short-time and long-time regions, indicating that the distribution of $\Delta x(t)$ shows a Gaussian distribution in these regions. On the other hand, it shows a peak in the intermediate time region, suggesting the presence of dynamic heterogeneity in this intermediate region.
- Furthermore, in Figure **7**, a comparison of $\alpha_2(t)$ with mean squared displacement is shown. It can be seen that $\alpha_2(t)$ peaks around the time region where the plateau of mean squared displacement ends and transitions to relaxation.

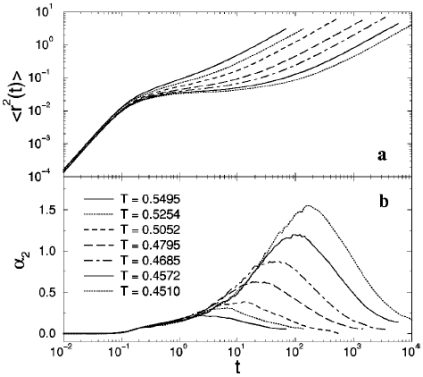

Fig. 7: Mean squared displacement and non-Gaussian parameter [11].

3.4. Dynamic Liquid Theory: Mean Squared Displacement, Intermediate Scattering Function, Non-Gaussian Parameter, Four-Point Correlation (14)

Report Assignment (4)

Derive that for the two-dimensional displacement vector $\Delta r(t)$, the non-Gaussian parameter is

$$\alpha_2(t) = \frac{\left\langle \Delta \mathbf{r}(t)^4 \right\rangle}{2\left\langle \Delta \mathbf{r}(t)^2 \right\rangle^2} - 1. \tag{36}$$

3.4. Dynamic Liquid Theory: Mean Squared Displacement, Intermediate Scattering Function, Non-Gaussian Parameter, Four-Point Correlation (15)

♣ Four-Point Correlation Function [12]

In supercooled liquids, heterogeneity arises in particle motion (dynamics), and it is known that with the glass transition, the spatial length scale increases as if it were a critical phenomenon (Fig. **8**). This property is called dynamic heterogeneity and is considered a factor in the sharp increase in viscosity at the glass transition point [13, 14].

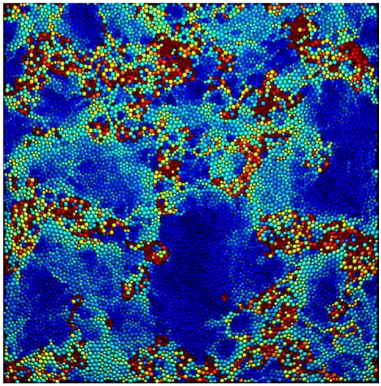

Fig. 8: Dynamic heterogeneity (spatial distribution of particle displacements in supercooled liquid) [15].

3.4. Dynamic Liquid Theory: Mean Squared Displacement, Intermediate Scattering Function, Non-Gaussian Parameter, Four-Point Correlation (16)

- To quantify dynamic heterogeneity, the most fundamental quantity defined is the overlap function. The overlap function can be defined for each particle, where it returns 0 if the displacement magnitude of particle j over the time interval $[t_0, t_0 + t]$ is larger than a, and 1 if smaller:

$$w_j(t_0 + t, t_0) = \Theta(a - |\Delta \mathbf{r}_j(t)|), \tag{37}$$

  where $\Theta(x)$ is the Heaviside step function, $\Theta(x) = 1$ for $x > 0$, and $\Theta(x) = 0$ otherwise.

- Next, the density field at time t_0 weighted by the overlap function over the time interval $[t_0, t_0 + t]$ is defined as

$$\rho_w(\mathbf{r}; t_0 + t, t_0) = \sum_{j=1}^{N} w_j(t_0 + t, t_0)\delta(\mathbf{r} - \mathbf{r}_j(t_0)), \tag{38}$$

  and the fluctuation is

$$\delta\rho_w(\mathbf{r}; t_0 + t, t_0) = \sum_{j=1}^{N} w_j(t_0 + t, t_0)\delta(\mathbf{r} - \mathbf{r}_j(t_0)) - \left\langle \frac{\sum_{j=1}^{N} w_j(t_0 + t, t_0)}{V} \right\rangle. \tag{39}$$

3.4. Dynamic Liquid Theory: Mean Squared Displacement, Intermediate Scattering Function, Non-Gaussian Parameter, Four-Point Correlation (17)

- The spatial Fourier transform of $\delta\rho_w$ is

$$\delta\tilde{\rho}_w(\mathbf{q};t_0+t,t_0)=\sum_{j=1}^{N}w_j(t_0+t,t_0)e^{-i\mathbf{q}\cdot\mathbf{r}_j}-\left\langle\sum_{j=1}^{N}w_j(t_0+t,t_0)\right\rangle\delta_{\mathbf{q},\mathbf{0}}, \tag{40}$$

where note that $\int_V d\mathbf{r}e^{-i\mathbf{q}\cdot\mathbf{r}}=V\delta_{\mathbf{q},\mathbf{0}}$.
Now, the structure factor related to $\delta\rho_w$ is defined as

$$\boxed{S_4(\mathbf{q};t_0+t,t_0)=\frac{1}{N}\left\langle\delta\tilde{\rho}_w(\mathbf{q};t_0+t,t_0)\delta\tilde{\rho}_w(-\mathbf{q};t_0+t,t_0)\right\rangle}, \tag{41}$$

which is useful for spatial structure analysis of the overlap field (dynamic heterogeneity).

3.4. Dynamic Liquid Theory: Mean Squared Displacement, Intermediate Scattering Function, Non-Gaussian Parameter, Four-Point Correlation (18)

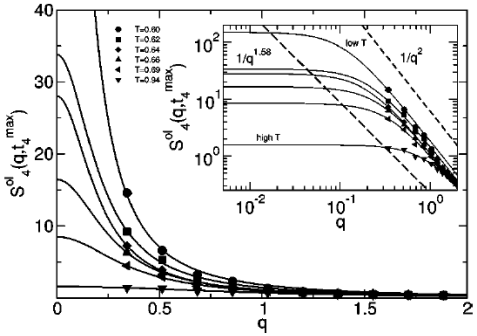

Fig. 9: Temperature dependence of $S_4(q; t_4^{max})$ in a supercooled liquid [12]. t_4^{max} is the time when $\chi_4(t)$ shows its maximum value.

3.4. Dynamic Liquid Theory: Mean Squared Displacement, Intermediate Scattering Function, Non-Gaussian Parameter, Four-Point Correlation (19)

- As shown in Fig. **9**, in typical S_4 analysis, the low wave number region is the focus. Particularly when there are heterogeneous fluctuations, $S_4(\mathbf{q}; t_0 + t, t_0)$ can be expressed by the Ornstein-Zernike function:

$$\boxed{S_4(q; t_0 + t, t_0) \sim \frac{S_{40}}{1 + (q\xi_4)^2}}, \tag{42}$$

  from which the correlation length ξ_4 can be calculated. The Ornstein-Zernike function represents the structure factor in a disordered phase (assuming free energy consisting of ϕ^2 and $(\nabla\phi)^2$) in Landau theory (mean-field theory) [16].
- Here, $S_{40} = S_4(0; t_0 + t, t_0)$ represents macroscopic fluctuations. Similar to the static structure factor,

$$\boxed{S_4(0; t_0 + t, t_0) = \rho k_B T \chi_4(t)}, \tag{43}$$

  defines the susceptibility $\chi_4(t)$. $\chi_4(t)$, written using the overlap function, is expressed as

$$\boxed{\chi_4(t) = \frac{V}{k_B T} \left\langle \left(\sum_{j=1}^{N} w_j(t + t_0, t_0) - \left\langle \sum_{j=1}^{N} w_j(t + t_0, t_0) \right\rangle \right)^2 \right\rangle}. \tag{44}$$

3.4. Dynamic Liquid Theory: Mean Squared Displacement, Intermediate Scattering Function, Non-Gaussian Parameter, Four-Point Correlation (20)

- Figure **10** (left) shows the temperature dependence of $\chi_4(t)$ in a supercooled liquid [12]. As the temperature decreases, the peak value becomes larger (indicating more heterogeneity), and the time at which the peak occurs becomes later (indicating slower relaxation).
- Figure **10** (right) shows the dynamic correlation length ξ_4. It varies depending on how the overlap time is taken. Particularly, for each temperature, $\xi_4(t)$ is maximized at the time when $\chi_4(t)$ peaks. Furthermore, as the temperature decreases, the increase in $\xi_4(t)$ (i.e., the increase in dynamic heterogeneity) can be observed.
- The origin of dynamic heterogeneity (such as the presence or absence of local structures) has been extensively studied up to the present day, but the understanding of universal properties has not yet been achieved. Recently, machine learning has been introduced to address this problem [17, 18, 19, 20, 21, 22, 23].

3.4. Dynamic Liquid Theory: Mean Squared Displacement, Intermediate Scattering Function, Non-Gaussian Parameter, Four-Point Correlation (21)

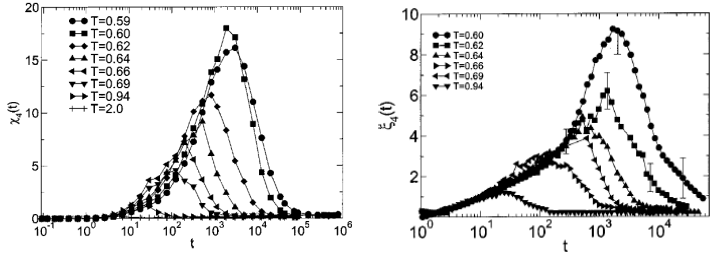

Fig. 10: (Left) Temperature dependence of $\chi_4(t)$ in a supercooled liquid. (Right) Changes in ξ_4 of the corresponding system. Reproduced from [12].

3.5. Summary

Summary of Glass Transition

- The glass transition is a universal phenomenon observed in various materials.
- Two-body density correlation functions do not capture the characteristics of the transition.
- The diffusion coefficient and structural relaxation time tend to diverge as the transition point approaches.
- The spatial distribution of dynamics becomes heterogeneous with glass formation.
- There have been attempts to understand the glass transition through analogies with critical phenomena (though still unresolved).

Contents

Section 4

Jamming Transition

4. Jamming Transition

♣ Jamming Transition [24]

Compression of athermal particles (granular materials) ($d \sim 10\ \mu\mathrm{m}$):

- Flow phase to (amorphous) solid phase transition: Jamming transition
- Nonequilibrium critical phenomena are observed at the jamming transition point.
- Although similar to the glass transition, it is known to be qualitatively different [25, 26].

In this lecture, we will show the above properties **as analytically as possible**, incorporating the latest research results.

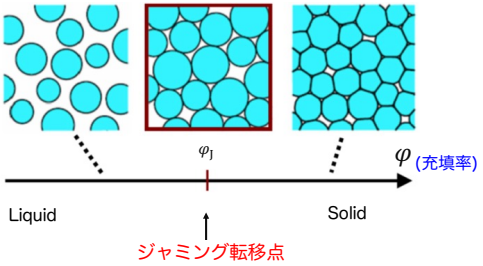

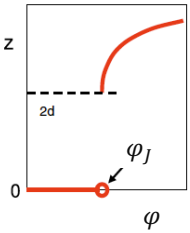

Fig. 11: Conceptual diagram of the jamming transition. In the low-density region, there are no contacts between particles. On the other hand, at $\varphi > \varphi_J$ (φ_J: jamming transition point), particle contacts and macroscopic rigidity are obtained. [24]

4.1. Interparticle Interactions in Jamming Systems

♣ Interparticle Interactions in Jamming Systems [27, 28]

- Particles in systems exhibiting jamming transitions can often be regarded as elastic spheres. The interaction between elastic spheres is known as Hertzian elastic theory and is expressed as follows [27, 28]:

$$U(r_{jk}) = \epsilon\left(1 - \frac{r_{jk}}{d_{jk}}\right)^{\alpha} \Theta(d_{jk} - r_{jk}) = \epsilon(\Delta_{jk}/d_{jk})^{\alpha}\Theta(-\Delta_{jk}). \tag{45}$$

  Here, $r_{jk} = |\mathbf{r}_j - \mathbf{r}_k|$, $d_{jk} = \frac{d_j + d_k}{2}$, and d_k, d_j are the diameters of particles k, j. Also, $\delta_{jk} = r_{jk} - d_{jk}$ is the overlap length between particles j and k, and $\Theta(d_{jk} - r_{jk})$ is the Heaviside step function, indicating that interaction occurs only when there is overlap.
- The exponent α of the potential is $\alpha = 5/2$ for elastic materials.
- For **inelastic materials, the value may differ**. Therefore, in the following discussion, we proceed using a general α.
- An important aspect of the jamming transition is that, **unlike ordinary thermodynamic phase transitions**, the exponent α of the potential appears in various critical phenomena shown below.

4.2. Criticality of Mechanical Variables

♣ Criticality of Mechanical Variables

- As shown in Fig. **12**, in a particle system near the jamming transition point, criticality appears in mechanical variables such as pressure P and shear modulus G (expressible as functions of $\delta\varphi = \varphi - \varphi_{\rm J}$) [24, 29, 30, 31].
- Mechanical variables exhibit critical behavior summarized below:

Critical Behavior of Mechanical Variables

- Potential Energy
$$U \sim \delta\phi^{\alpha} \tag{46}$$
- Pressure
$$P \sim \delta\phi^{\alpha-1} \tag{47}$$
- Bulk Modulus
$$B \sim \delta\phi^{\alpha-2} \tag{48}$$
- Shear Modulus
$$G \sim \delta\phi^{\alpha-3/2} \tag{49}$$

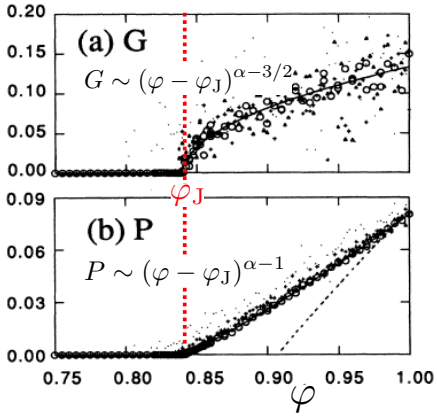

Fig. 12: Criticality of mechanical variables associated with the jamming transition [29]

4.2. Criticality of Mechanical Variables (2)

Below, we roughly prove the above critical phenomena.

- Let the system volume be V, the number of particles be N, and the diameter of each particle be d (for simplicity, all are of the same size). At this time, the volume fraction of particles is

$$\phi = \frac{\pi N}{6V} d^3. \tag{50}$$

- By changing the size of the particles, we change ϕ. At this time, if the particle diameter at the jamming point is d_J, then

$$\varphi_\mathrm{J} = \frac{\pi N}{6V} d_\mathrm{J}^3. \tag{51}$$

- Now, let $\phi = \varphi_\mathrm{J} + \delta\phi$, and if the diameter of each particle at this time is $d_J + \Delta$, then Δ corresponds to the overlap length in Fig. **13**, and assuming $\Delta \ll 1$, we have

$$\phi = \varphi_\mathrm{J} + \delta\varphi = \frac{\pi N}{6V}(d_\mathrm{J} + \Delta)^3 \sim \varphi_\mathrm{J}(1 + 3\Delta/d_\mathrm{J}). \tag{52}$$

- Therefore, we obtain the relationship between the small quantity $\delta\phi$ and Δ as follows:

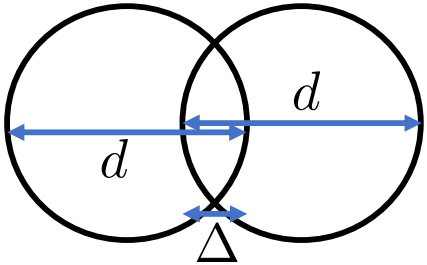

Fig. 13: Overlap Δ between particles

4.2. Criticality of Mechanical Variables (3)

- From this, the potential energy is $U \propto \Delta^\alpha$, so

$$\boxed{U \propto \Delta^\alpha \propto \delta\phi^\alpha.} \tag{54}$$

- The pressure, with the force on each particle being F, is approximately $P \sim \rho F d$ from the Virial theorem, so

$$\boxed{P \propto F \sim \frac{\partial U}{\partial r} \sim \frac{\partial U}{\partial \Delta} \propto \Delta^{\alpha-1} \propto \delta\phi^{\alpha-1}.} \tag{55}$$

- The bulk modulus B is $B = -\frac{\partial P}{\partial V}$. Now,

$$\varphi_J + \delta\varphi = \frac{\pi N}{6(V-\delta V)} d_J^3 \sim \varphi_J(1 - \frac{\delta V}{V}), \tag{56}$$

so since $\delta\varphi \propto \delta V$,

$$\boxed{B \sim \frac{\partial P}{\partial(\delta\phi)} \propto \delta\phi^{\alpha-2}.} \tag{57}$$

- The shear modulus G, for shear strain γ, is $G \sim \frac{\partial^2 U}{\partial \gamma^2}$. In shear deformation, note that rigidity is borne by the excess contacts from the marginally stable point.

4.2. Criticality of Mechanical Variables (4)

- The number of contacts in the isostatic state (jamming transition point) showing marginal stability is $\boxed{Z_c = 2d}$ **(to be proven later)**.
- If the number of excess contacts is δZ, the number of contacts at $\phi \geq \varphi_J$ is $Z = Z_c + \delta Z$.
- δZ is $\boxed{\delta Z \propto \sqrt{\delta\phi}}$ **regardless of α (to be proven later)** [29, 30].
- In shear deformation, there is no volume change, so the rigidity is contributed by δZ contact points per particle.
- The order of rigidity per contact (corresponding to the spring constant in particle bonding) is $k = B/N \propto \delta\phi^{\alpha-2}$, so

$$\boxed{G \sim (\delta Z)k \propto \delta\phi^{\alpha-3/2}}. \tag{58}$$

4.3. Marginal Stability and Criticality of the Number of Interparticle Contacts

♣ Marginal Stability of the Number of Interparticle Contacts: $\boxed{Z_c = 2d}$

At the jamming transition point, the particle structure (number of contacts) reaches a marginally stable state $Z_c = 2d$.

Definition of the Jamming Transition Point

1. Marginal stability
2. Interparticle overlap $= 0$

Condition $\boxed{1}$:

- For a d-dimensional particle structure to be stable against a small external force,
  $\boxed{\text{the number of degrees of freedom of particles} \leq \text{number of constraints between particles}}$.

4.3. Marginal Stability and Criticality of the Number of Interparticle Contacts (2)

- Now, the number of degrees of freedom of particles and the number of constraints between particles are respectively

$$\text{Number of degrees of freedom of particles} = dN \tag{59}$$

$$\text{Number of constraints between particles} = \frac{ZN}{2}. \tag{60}$$

Therefore, the stability condition against a small external force is

$$dN \leq \frac{ZN}{2}, \tag{61}$$

that is,

$$\boxed{Z \geq 2d}. \tag{62}$$

Condition $\boxed{2}$:

- If the number of degrees of freedom of particles $\geq$ the number of constraints between particles, all interparticle contacts can be resolved in a stable state.
- At this time,

$$\boxed{Z \leq 2d}. \tag{63}$$

4.3. Marginal Stability and Criticality of the Number of Interparticle Contacts (3)

From conditions 1 and 2, the number of interparticle contacts Z_c at the jamming transition point is

$$\boxed{Z_c = 2d}. \tag{64}$$

4.4. Excess Contact Number and Cutting Argument

♣ Cutting Argument [32, 33]

Below, using a method called the cutting argument, we analytically demonstrate the criticality of the excess contact number $\boxed{\delta Z \propto \sqrt{\delta\phi}}$.

- First, prepare a sufficiently large solid system in a stable state, with $\phi \geq \varphi_J$ (Fig. **14** top).
- At this time, the number of interparticle contacts per particle is $Z = Z_c + \delta Z$.
- Now, cut out a spherical region (cluster) of diameter ℓ and remove the surrounding particles.
- Then, the particles start to move and stop when forces are balanced (Fig. **14** bottom).

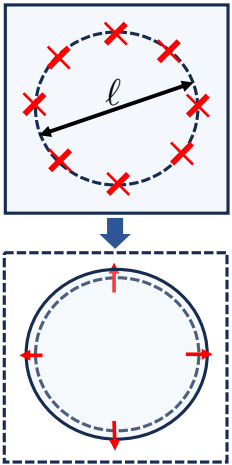

Fig. 14: Cutting argument: Cutting out a cluster of diameter ℓ.

4.4. Excess Contact Number and Cutting Argument (2)

♣ Condition for the Cut-Out Cluster to Maintain Stability

Next, consider the conditions (Marginal stability conditions) for a cut-out cluster of diameter ℓ to maintain a solid stable state (jamming state).

- When cut out, the number of bonds lost by the cluster is proportional to the surface area of the cluster, so $\sim \ell^2$.
- The total excess contact number of the cluster before cutting is proportional to the volume of the cluster, so $\sim \ell^3 \delta Z$.
- If the total excess contact number exceeds the number of bonds lost, the cut-out cluster is stable, so the stability condition is

$$\ell^3 \delta Z \geq \ell^2. \tag{65}$$

  Thus,

$$\ell \geq \frac{1}{\delta Z}, \tag{66}$$

  the cluster satisfies this condition and can maintain a stable jamming solid state.
- In a sufficiently large jamming solid, plane waves with wavelength $\lambda \geq \frac{1}{\delta Z}$ are stable. Waves with shorter wavelengths are soft modes.
- The marginal stability size of the jamming solid is

$$\boxed{\ell^* = \frac{1}{\delta Z}}. \tag{67}$$

4.4. Excess Contact Number and Cutting Argument (3)

♣ Relaxation Process of a Cut-Out Cluster at Marginal Stability [Original]

(1) Orthogonal Decomposition of Particle Displacement

- Let the displacements of particles j and k be $\mathbf{u}_j$ and $\mathbf{u}_k$, respectively.
- The displacement of particle j relative to particle k (relative displacement) is $\mathbf{u}_{jk} = \mathbf{u}_j - \mathbf{u}_k$.
- The bond vector between particles j and k is $\mathbf{n}_{jk} = \frac{\mathbf{r}_{jk}}{r_{jk}}$.
- The parallel and perpendicular components of $\mathbf{u}_{jk}$ relative to $\mathbf{n}_{jk}$ are respectively

$$\begin{aligned} \mathbf{u}_{jk}^{\parallel} &= (\mathbf{u}_{jk}\cdot\mathbf{n}_{jk})\mathbf{n}_{jk} \\ &= (\mathbf{n}_{jk}\otimes\mathbf{n}_{jk})\cdot\mathbf{u}_{jk}, \end{aligned} \tag{68}$$

$$\begin{aligned} \mathbf{u}_{jk}^{\perp} &= \mathbf{u}_{jk} - (\mathbf{u}_{jk}\cdot\mathbf{n}_{jk})\mathbf{n}_{jk} \\ &= (\mathbf{1} - \mathbf{n}_{jk}\otimes\mathbf{n}_{jk})\cdot\mathbf{u}_{jk}, \end{aligned} \tag{69}$$

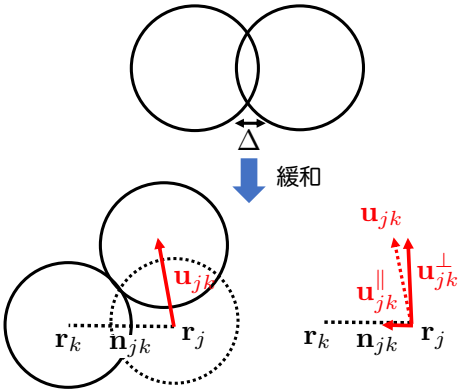

Fig. 15: Relaxation dynamics after cutting. The relative displacement $\mathbf{u}_{jk}$ of particles j and k is decomposed into the parallel component $\mathbf{u}_{jk}^{\parallel}$ and the perpendicular component $\mathbf{u}_{jk}^{\perp}$ relative to the bond vector $\mathbf{n}_{jk}$.

4.4. Excess Contact Number and Cutting Argument (4)

Calculation Notes (Component Calculations)

Equation (68):

$$u_\alpha^{\parallel} = \sum_\beta (u_\beta n_\beta) n_\alpha = \sum_\beta (n_\beta n_\alpha) u_\beta,$$

so

$$\mathbf{u}^{\parallel} = (\mathbf{n} \otimes \mathbf{n}) \cdot \mathbf{u}.$$

Equation (69):

$$\begin{aligned} u_\alpha^{\perp} &= u_\alpha - \sum_\beta u_\beta n_\beta n_\alpha \\ &= \sum_\beta (\delta_{\alpha\beta} u_\beta - u_\beta n_\beta n_\alpha) \\ &= \sum_\beta (\delta_{\alpha\beta} - n_\alpha n_\beta) u_\beta, \end{aligned}$$

where $\{\delta_{\alpha\beta}\}$ is the $\alpha\beta$ component of the identity matrix. Thus,

$$\mathbf{u}^{\perp} = (\mathbf{1} - \mathbf{n} \otimes \mathbf{n}) \cdot \mathbf{u}.$$

4.4. Excess Contact Number and Cutting Argument (5)

(2) Relationship between Orthogonally Decomposed Relative Displace

Here, we evaluate the relationship between orthogonally decomposed relative displacements $u_{jk}^{\parallel}$, $u_{jk}^{\perp}$ and Δ ($\delta\phi$) (Fig. **16**).

Parallel Component

- As shown in Fig. **16** (top), relax the overlap Δ in the parallel direction, so

$$u_{jk}^{\parallel} \sim \Delta \sim \delta\phi. \tag{70}$$

Perpendicular Component

- Focusing on the right triangle in Fig. **16** (bottom), from the Pythagorean theorem,

$$\begin{aligned} u_{jk}^{\perp} &= \sqrt{d^2 - (d-\Delta)^2} \sim \sqrt{2d\Delta - \Delta^2} \\ &\sim \sqrt{\Delta} \sim \sqrt{\delta\phi}. \end{aligned} \tag{71}$$

For $\varphi \ll 1$, $u_{jk}^{\perp} \gg u_{jk}^{\parallel}$. Such a perpendicular component $u_{jk}^{\perp}$ is called a floppy mode.

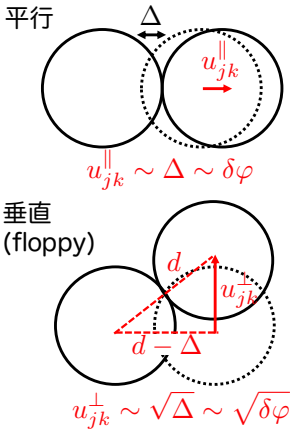

Fig. 16: Relationship between orthogonally decomposed relative displacement and overlap Δ ($\delta\phi$).

4.4. Excess Contact Number and Cutting Argument (6)

(3) Potential Energy Relaxation

Here, we consider the energy relaxation of the cut-out cluster.

- Let the set of relative displacements during relaxation be $\{\mathbf{u_{jk}}\}$.
- Let the set of relative coordinates at the starting point of relaxation be $\{\mathbf{r}_{jk}\}$ and at the endpoint be $\{\mathbf{r}_{jk}+\mathbf{u}_{jk}\}$.
- Expanding the potential energy at the endpoint $U(\{\mathbf{r}_{jk}+\mathbf{u}_{jk}\})$ around the starting point $U(\{\mathbf{r}_{jk}\})$ to the second order [24, 34], we get

$$
\begin{aligned}
U(\{\mathbf{r}_{jk}+\mathbf{u}_{jk}\}) &\sim U(\{\mathbf{r}_{jk}\}) + \sum_{\langle jk\rangle} \frac{\partial U(\{\mathbf{r}_{jk}\})}{\partial \mathbf{r}_{jk}} \cdot \mathbf{u}_{jk} + \frac{1}{2}\sum_{\langle jk\rangle} \mathbf{u}_{jk} \cdot \frac{\partial^2 U(\{\mathbf{r}\})}{\partial \mathbf{r}_{jk}\partial \mathbf{r}_{jk}} \cdot \mathbf{u}_{jk} \\
&\sim U(\{\mathbf{r}_{jk}\}) - \sum_{\langle jk\rangle} \mathbf{F}_{jk} \cdot \mathbf{u}_{jk} - \frac{1}{2}\sum_{\langle jk\rangle} \mathbf{u}_{jk} \cdot \frac{\partial \mathbf{F}_{jk}}{\partial \mathbf{r}_{jk}} \cdot \mathbf{u}_{jk} \\
&\sim U(\{\mathbf{r}_{jk}\}) - \sum_{\langle jk\rangle} F_{jk}\mathbf{n}_{jk} \cdot \mathbf{u}_{jk} - \frac{1}{2}\sum_{\langle jk\rangle} \mathbf{u}_{jk} \cdot \left\{ (\mathbf{n}_{jk}\otimes\mathbf{n}_{jk})\frac{\partial F_{jk}}{\partial r_{jk}} + \frac{(\mathbf{1}-\mathbf{n}_{jk}\otimes\mathbf{n}_{jk})}{r_{jk}} F_{jk} \right\} \cdot \mathbf{u}_{jk} \\
&\sim U(\{\mathbf{r}_{jk}\}) - \sum_{\langle jk\rangle} F_{jk} u_{jk}^{\parallel} - \frac{1}{2}\sum_{\langle jk\rangle} \left\{ \frac{\partial F_{jk}}{\partial r_{jk}} (u_{jk}^{\parallel})^2 + \frac{F_{jk}}{r_{jk}} (u_{jk}^{\perp})^2 \right\}. \qquad (72)
\end{aligned}
$$

4.4. Excess Contact Number and Cutting Argument (7)

Report Assignment (5)

Follow the calculation process of Equation (72).

- Now, the potential energy at the starting point is $\boxed{U(\{\mathbf{r}_{jk}\}) \sim (\ell^*)^3 \delta\varphi^\alpha}$, and at the endpoint, $\Delta Z \to 0$ and the configuration at the jamming point is reached, so $\boxed{U(\{\mathbf{r}_{jk} + \mathbf{u}_{jk}\}) = 0}$. Therefore, Equation (72) is

$$(\ell^*)^3 \delta\varphi^\alpha \sim \sum_{\langle jk \rangle} F_{jk} u^{\parallel}_{jk} + \frac{1}{2} \sum_{\langle jk \rangle} \left\{ \frac{\partial F_{jk}}{\partial r_{jk}} (u^{\parallel}_{jk})^2 + \frac{F_{jk}}{r_{jk}} (u^{\perp}_{jk})^2 \right\}. \tag{73}$$

  Now, $\sum_{\langle jk \rangle} \sim (\ell^*)^3 Z$. Therefore, generally writing the contribution per particle,

$$\delta\varphi^\alpha \sim F u^{\parallel} + \frac{1}{2} \left\{ \frac{\partial F}{\partial r} (u^{\parallel})^2 + \frac{F}{r} (u^{\perp})^2 \right\}. \tag{74}$$

- Here, $F \propto \delta\phi^{\alpha-1}$, $\frac{\partial F}{\partial r} \propto \delta\phi^{\alpha-2}$.

4.4. Excess Contact Number and Cutting Argument (8)

- Assuming all terms on the right side of Equation (74) contribute to $\delta\phi^\alpha$, including the average values $u^\parallel$ and $u^\perp$ of the cut-out cluster boundary contributions,

$$u^\parallel \sim \delta\varphi, \quad u^\perp \sim \sqrt{\delta\varphi}. \tag{75}$$

(4) Contribution of Boundary Particles to Energy Relaxation

- In subsection (2), the relative displacement in the bulk region was estimated as

$$u^\parallel_{jk} \sim \delta\varphi, \quad u^\perp_{jk} \sim \sqrt{\delta\varphi}. \tag{76}$$

  The magnitude of the perpendicular component $\sqrt{\delta\varphi}$ corresponds to a floppy mode.
- However, when the cut-out cluster relaxes, if we assume that both the perpendicular and parallel components become floppy in the boundary region (approximately $(\ell^*)^2$ particles) (Fig. **17**),

$$u^{\parallel(\mathrm{bound})}_{jk} \sim \sqrt{\delta\varphi}, \quad u^{\perp(\mathrm{bound})}_{jk} \sim \sqrt{\delta\varphi}. \tag{77}$$

4.4. Excess Contact Number and Cutting Argument (9)

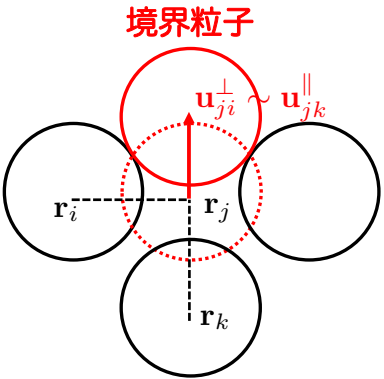

Fig. 17: Boundary particles of a cut-out jamming solid also exhibit floppy displacements in the perpendicular component. Here, when a boundary-lost particle j moves, since $\mathbf{u}_{ji}^{\perp} \sim \mathbf{u}_{jk}^{\parallel}$, the estimate in Equation (77) is considered valid.

4.4. Excess Contact Number and Cutting Argument (10)

Therefore, estimating the average values considering these contributions, the perpendicular component is straightforward, but for the parallel component, from Equations (75), (76), and (77),

$$u^{\parallel} \propto \delta\varphi \quad \propto \quad \frac{1}{(\ell^*)^3}\left\{\underbrace{(\ell^*)^2\sqrt{\delta\varphi}}_{\text{boundary}} + \underbrace{(\ell^*)^3\delta\varphi}_{\text{bulk}}\right\} \sim \frac{\sqrt{\delta\varphi}}{\ell^*} + \delta\varphi. \tag{78}$$

Thus,

$$\frac{\sqrt{\delta\varphi}}{\ell^*} \propto \delta\varphi, \tag{79}$$

that is,

$$\boxed{\ell^* \propto \frac{1}{\sqrt{\delta\varphi}}}. \tag{80}$$

Finally, from Equation (67): $\ell^* \propto \frac{1}{\delta Z}$,

$$\boxed{\delta Z \propto \sqrt{\delta\varphi}} \tag{81}$$

is obtained (Fig. **18**).

4.4. Excess Contact Number and Cutting Argument (11)

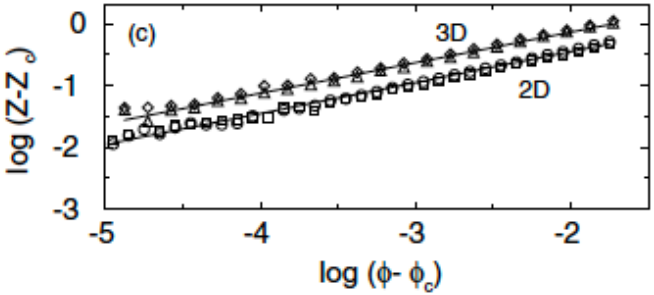

Fig. 18: Criticality of excess contact number δZ near the jamming transition point [30].

4.4. Excess Contact Number and Cutting Argument (12)

(5) Derivation of Vibrational Density of States in Jamming System

- At the jamming transition point, a soft mode with a vibrational density of states $D(\omega) \sim \text{const}$ is observed [32].
- For $\varphi > \varphi_J$, a plane wave mode is observed for $\omega < \omega^*$, and a soft mode is observed for $\omega > \omega^*$ (Fig. **19**).
- Below, using insights from the cutting argument in previous sections, we derive the criticality of $D(\omega) \sim \text{const}$ and $\omega < \omega^*$ at the jamming point.
- First, for $\varphi > \varphi_J$, plane waves with wavelengths shorter than the marginal stability size ℓ^* of the solid corresponding to this density do not exist. Therefore, from the linear dispersion relation $\omega = ck \propto 1/\lambda$,

$$\omega^* \propto \frac{1}{\ell^*} \sim \delta z \sim \sqrt{\delta\varphi}. \qquad (82)$$

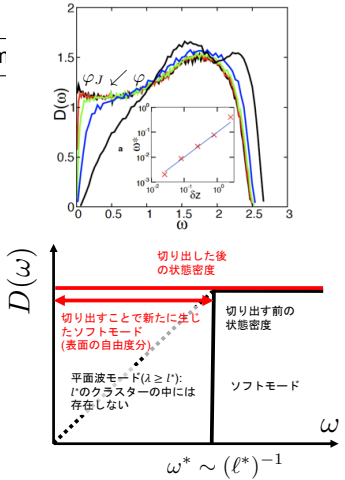

Fig. 19: Vibrational density of states $D(\omega)$ near the jamming transition point. (Top) Simulation results [32]. (Bottom) Schematic diagram.

4.4. Excess Contact Number and Cutting Argument (13)

- When cutting out a solid of size ℓ^*, new soft modes appear in the $\omega < \omega^*$ region of Fig. **19**.
- These soft modes are considered to contribute to the degrees of freedom of the boundary $(\ell^*)^2$ when cut out.
- Let the vibrational density of states per unit volume related to soft modes at the jamming point be $D(\omega) = \omega^x$, then

$$(\ell^*)^3 \int_0^{1/\ell^*} d\omega D(\omega) = (\ell^*)^2. \tag{83}$$

Therefore,

$$(\ell^*)^3 (1/\ell^*)^{x+1} = (\ell^*)^2, \tag{84}$$

gives $x = 0$, so

$$\boxed{D(\omega) \sim \text{const}}. \tag{85}$$

is derived.

4.5. Nonlinear Rheology of Jamming Systems

- Near the jamming transition point, a non-trivial nonlinear rheology (softening) is observed in response to a small strain (Fig. **20**) [35, 36, 37].
- Details of various criticalities in the elastic region, softening region, and yielding region will be explained in a separate slide.

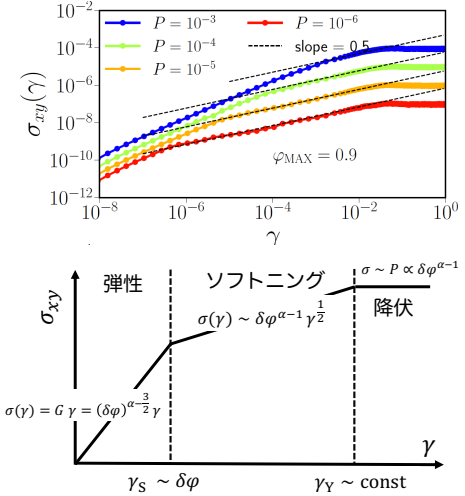

Fig. 20: Stress-strain curve near the jamming transition point. Near the transition point, a nonlinear rheology called softening is observed. (Top) Simulation results. Pressure dependence. The lower the pressure, the closer it is to the jamming

4.6. Summary

Summary of Jamming Transition

- The jamming transition is observed in systems of large particles where thermal motion can be ignored.
- The jamming transition is similar to the glass transition but is essentially a different transition.
- In the jamming transition, mechanical variables such as the number of interparticle contacts show clear criticality.
- By discussing the stability of finite volume solids near the jamming point, the criticality of the number of interparticle contacts and vibrational density of states can be understood.
- Nonlinear rheology called softening is observed near the jamming point.

Contents

Section 5

Nonlinear Rheology of Colloidal Dispersions

5. Nonlinear Rheology of Colloidal Dispersions

Nonlinear rheology of colloidal dispersions will be explained in a separate slide [25, 38, 39].

Contents

References

[1] V. Regnault,
Annalen der Physik **174**, 396 (1856).

[2] C. A. Angell,
Science **267**, 1924 (1995).

[3] P. G. Debenedetti and F. H. Stillinger,
Nature **410**, 259 (2001).

[4] C. A. Angell,
Journal of Physics and Chemistry of Solids **49**, 863 (1988).

[5] Jean-Pierre Hansen and I. McDonald,
Theory of Simple Liquids - 4th Edition,
Elsevier, Acad. Press.

[6] T. M. Truskett, S. Torquato, S. Sastry, P. G. Debenedetti, and F. H. Stillinger,
Phys. Rev. E **58**, 3083 (1998).

[7] W. Kob and H. C. Andersen,
Phys. Rev. E **51**, 4626 (1995).

References (2)

[8] H. B. Callen,
Thermodynamics and an Introduction to Thermostatistics,
John Wiley & Sons, 1991.

[9] W. Kob and H. C. Andersen,
Phys. Rev. Lett. **73**, 1376 (1994).

[10] A. Rahman,
Phys. Rev. **136**, A405 (1964).

[11] C. Donati, S. C. Glotzer, P. H. Poole, W. Kob, and S. J. Plimpton,
Phys. Rev. E **60**, 3107 (1999).

[12] N. Lačević, F. W. Starr, T. B. Schrøder, and S. C. Glotzer,
The Journal of Chemical Physics **119**, 7372 (2003).

[13] R. Yamamoto and A. Onuki,
Phys. Rev. Lett. **81**, 4915 (1998).

[14] W. Kob, C. Donati, S. J. Plimpton, P. H. Poole, and S. C. Glotzer,
Phys. Rev. Lett. **79**, 2827 (1997).

References (3)

[15] J. P. Garrahan,
Proceedings of the National Academy of Sciences **108**, 4701 (2011).

[16] Hidetoshi Nishimori and Gerardo Ortiz,
Elements of Phase Transitions and Critical Phenomena,
Oxford University Press.

[17] T. Kawasaki, T. Araki, and H. Tanaka,
Phys. Rev. Lett. **99**, 215701 (2007).

[18] H. Tanaka, T. Kawasaki, H. Shintani, and K. Watanabe,
Nat Mater **9**, 324 (2010).

[19] V. Bapst et al.,
Nature Physics **16**, 448 (2020).

[20] E. Boattini, M. Dijkstra, and L. Filion,
The Journal of Chemical Physics **151**, 154901 (2019).

[21] E. Boattini et al.,
Nature Communications **11**, 5479 (2020).

References (4)

[22] E. Boattini, F. Smallenburg, and L. Filion,
Phys. Rev. Lett. **127**, 088007 (2021).

[23] N. Oyama, T. Kawasaki, and K. Saitoh,
Front. Phys. **9** (2021).

[24] M. van Hecke,
J. Phys.: Condens. Matter **22**, 033101 (2010).

[25] A. Ikeda, L. Berthier, and P. Sollich,
Phys. Rev. Lett. **109**, 018301 (2012).

[26] A. Ikeda, L. Berthier, and P. Sollich,
Soft Matter **9**, 7669 (2013).

[27] L. D. Landau, E. M. Lifshits, A. M. Kosevich, and L. P. Pitaevskii,
Theory of Elasticity: Volume 7,
Elsevier, 1986.

[28] V.L. Popov and 中野 健 訳,
接触と摩擦の物理学 (原著名：Contact Mechanics and Friction: Physical Principles and Applications, 2nd Ed),
丸善出版, 2023.

References (5)

[29] D. J. Durian,
Phys. Rev. Lett. **75**, 4780 (1995).

[30] C. S. O'Hern, S. A. Langer, A. J. Liu, and S. R. Nagel,
Phys. Rev. Lett. **88**, 075507 (2002).

[31] C. S. O'Hern, L. E. Silbert, A. J. Liu, and S. R. Nagel,
Phys. Rev. E **68**, 011306 (2003).

[32] M. Wyart, S. R. Nagel, and T. A. Witten,
EPL **72**, 486 (2005).

[33] M. Wyart,
Ann. Phys. Fr. **30**, 1 (2005).

[34] 別所秀将,
名古屋大学大学院理学研究科 2022 年度修士論文 .

[35] M. Otsuki and H. Hayakawa,
Phys. Rev. E **90**, 042202 (2014).

[36] J. Boschan, D. Vågberg, E. Somfai, and B. P. Tighe,
Soft Matter **12**, 5450 (2016).

References (6)

[37] S. Dagois-Bohy, E. Somfai, B. P. Tighe, and M. van Hecke,
Soft Matter **13**, 9036 (2017).

[38] T. Kawasaki, D. Coslovich, A. Ikeda, and L. Berthier,
Phys. Rev. E **91**, 012203 (2015).

[39] T. Kawasaki and L. Berthier,
Phys. Rev. E **98**, 012609 (2018).